17th World Conference on Earthquake Engineering, 17WCEE
Sendai, Japan - September 27th to October 2nd, 2021

NONLINEAR DYNAMIC ANALYSIS OF AN INFILLED RC FRAME BUILDING DURING THE 2016, MUISNE, ECUADOR EARTHQUAKE

P. Paredes[(1)], J. Romero[(2)]

[(1)] *MS graduate, University at Buffalo, pparedes@buffalo.edu*
[(2)] *MS graduate, University at Buffalo, jorgemig@buffalo.edu*

Abstract

This paper presents the response of a numerical model under seismic loading of a four-story building located in Portoviejo, Ecuador. The main focus of the analysis is the event of April 16th, 2016, where a MW 7.8 shallow megathrust faulting earthquake struck the coast of Ecuador. The maximum recorded PGA in Portoviejo was 0.38g, in the station APO1, which is located 1.2 km northwest of the case-study building. The structure was finished in 2011, which had served as an office building until the event. The building had interior partitions made of aluminum and gypsum. However, the perimeter walls were clay masonry infills, except in the front façade. To analyze the structure, a Tier 1 screening, and a Tier 3 systematic evaluation were developed following guidelines in ASCE 41-17. The nonlinear modeling of the structure was performed using OpenSees The material properties of the structure used in the model were collected after the earthquake by testing concrete cores for compressive strength, corrosion of the rebar, system identification of both the building and the soil to determine the natural period of both, geotechnical analysis of soil including site effect, and collecting information on the HVAC, water and electrical systems. Also, infill walls are accounted for in the analysis by following the recommendations for infilled RC frames proposed in ASCE 41-17. The general approach is to first classify each infilled frame of the structure as either ductile or nonductile based on a relation between the column shear strength and the shear force corresponding to the development of plastic hinges over the column. Later, the infill is categorized as relatively flexible or stiff based on the ratio of lateral stiffnesses of the column and infill. Depending on the above, a specific set of equations is used to calculate the yield, peak and residual strength, and drift of the infilled frames. The results from comparing the natural period of the structure after being subjected to the EQ in the analysis and the information provided by the post-earthquake testing match. Therefore, the state of the masonry infills is compared to validate the model by contrasting the actual damage state of the infill walls with the force-vs.-displacement responses of each element representing the infills in the model. The elements that represent the infill walls present a response that accurately describes the damage presented by the infills of the structure.

Keywords: ASCE 41 evaluation, nonlinear modeling, Muisne earthquake, masonry infilled RC frames, system ID.

1. Introduction

This paper presents the response of a numerical model under a specific seismic loading scenario of a four-story infilled RC frame building located in Portoviejo, Ecuador. The building may represent the typical construction practices for low-to-midrise buildings in Ecuador. The analysis focuses on the event of April 16th, 2016, where a MW 7.8 shallow megathrust faulting earthquake struck the central and northern coast of Ecuador. The building used light interior partitions, however, the perimeter frames, with the exception of the front façade, were infilled with clay masonry walls. The data collection process, as well as the identification of structural deficiencies and the nonlinear modeling of the building, were performed following the requirements of ASCE 41-17. The nonlinear modeling of the structure was done using OpenSees. The natural periods of the nonlinear model after being subjected to the 2016, Muisne earthquake were compared to the ambient vibration periods from the post-earthquake system identification. Finally, the force-vs.-displacement responses of the elements representing the infill walls in the model were contrasted with the actual damage state of the infills in the building. Other engineering demand parameters of the building were also extracted from the model to better understand the behavior of the structure during the earthquake.

2. The April 16th, 2016 Muisne Earthquake

On the evening of April 16th, 2016, a MW 7.8 shallow megathrust faulting earthquake struck the central and northern coast of Ecuador, causing extensive damage throughout the provinces of Esmeraldas, Manabi and Guayas. The final death toll was 668 and the losses amounted approximately $1.3 billion [1]. The maximum reported intensity according to the European Macro-seismic Scale (EMS-98) was IX [2]. The maximum PGA, 1.407 g, was recorded in the station APED, located 35 km south of the epicenter, in the city of Pedernales. The four-story building, which is the focus of this paper, is located in Portoviejo, Manabi, a city emplaced 167 km south of the epicenter of the 2016 Muisne earthquake. The maximum PGA in Portoviejo was 0.38g, recorded in the station APO1, located 1.2 km northwest of the case-study building.

3. Description of the case-study building

According to official figures presented by the Census Bureau of Ecuador [3], 94% of the buildings are built using reinforced concrete, being moment frames the almost exclusive structural system for low-to-midrise buildings. Moreover, it is of general practice to use unreinforced masonry walls as partitions, with 54% of the buildings using hollow concrete blocks and 44% of the buildings using clay bricks. Although not recognized as a structural system in the Ecuadorian Construction Standard [4], the resultant structures of a big portion of the buildings in Ecuador, can be easily categorized as Concrete Frames with Infill Masonry Shear Walls (C3), as in Table 3.1 of ASCE 41-17 [5].

The building analyzed finished construction in 2011, which is, five years before the Muisne earthquake. It was identified as an office building with light aluminum and gypsum office partitions in the interior. However, the lateral and back façades of the building were entirely infilled with masonry walls, composed of clay bricks without any reinforcement. The front façade was covered mainly with glass. Furthermore, the structure of the building is a four by four bay reinforced concrete moment frame. The span of the bays is approximately 4.45m. The perimeter frames of the lateral and back façades are considered concrete moment frames with infill masonry shear walls. The dimensions and reinforcement layout of columns, beams, slabs, and grade beams are shown in Table 1. A picture of the building, taken days after the 2016 Muisne earthquake, and the plan view are presented in Figure 1.

Table 1. Dimensions and reinforcement of structural elements

Element	Cross section (mm)	Longitudinal reinforcement	Transverse reinforcement
Columns	350x350 (300x300 in 4th story)	8φ14mm	Square and diamond closed hoops φ6mm@100mm in l_o, and φ6mm@200mm outside l_o.
Beams	500x250 (same height as the slab)	6φ14mm	φΦ6mm@100mm closed hoops
Waffle slab	h=250	1φ12mm@500mm	n/A
Grade beams	300x1000	Unknown	Unknown

It is of common practice in Ecuador to use waffle slabs as a floor system. The slabs are usually lightened by hollow concrete blocks, which are used as formwork with dimensions of 400x400x200mm . The lightweight blocks are left inside the slab once the concrete is poured, as it was the case in this building. The topping of the slab was 50mm or more, resulting in a minimum total height of 250mm. The ribs are 100mm in width. Another common practice in Ecuador, at least until the last decade, was the use of beams of the same depth of the slab, that is for this case, 250mm. The main reason for this practice is to simplify the formwork, resulting in a floor system similar to a flat slab. These beams are usually constructed wider than the columns. In the case-study building, beams are 500mm in width. Flipping the beam cross sections results in a significant reduction in inertia as compared to a typical moment frame system. Thus, this type of buildings tends to be flexible. However, the use of wide beams with transverse reinforcement helps, at least, to prevent punching shear failures in the slab system, depending on the design. As shown, this building exemplifies some of the common construction and design practices in Ecuador.

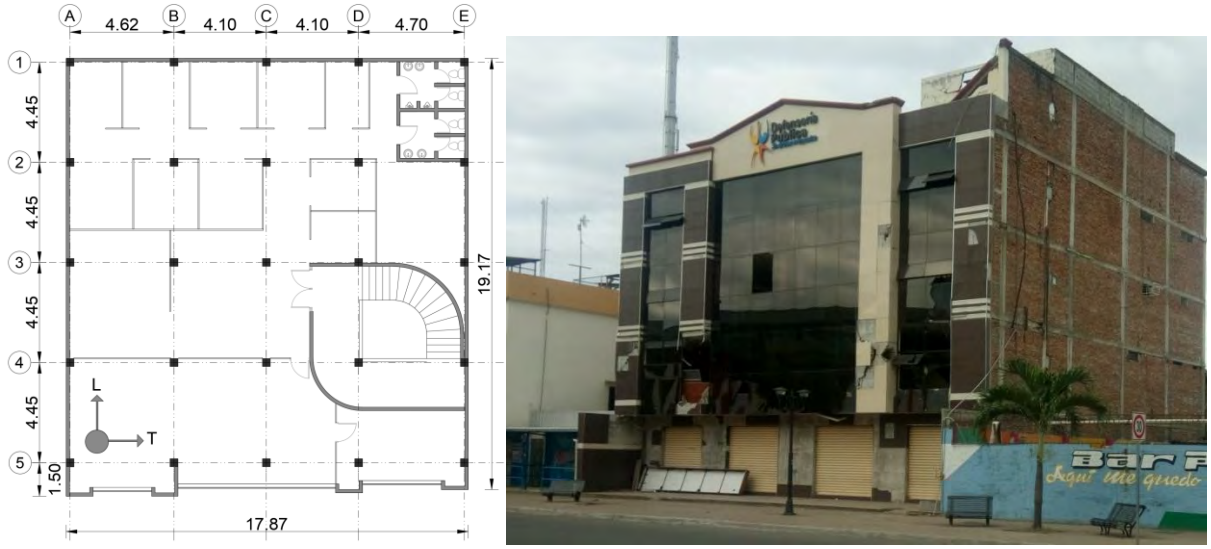

(a) (b)

Fig. 1 – (a) Typical Plan View, dimensions in meters (b) Photo of the building after the 2016, Muisne earthquake

4. Post-earthquake data collection following ASCE 41

The information described in this section was obtained in two consultancy contracts with the owner of the building, the first, in May 2016 (one month after the earthquake), and the second one year later, in May 2017. Both a Tier 1 screening and a Tier 3 systematic evaluation were carried out following ASCE 41. A comprehensive data collection was executed including concrete cores extraction and ultrasonic velocity

testing to evaluate the compressive strength of the concrete; determination of the dimensions and reinforcement of all of the structural elements; system identification of both the building and the soil; geotechnical investigation of the soil including site effect; determination of the potential of corrosion of the rebar; and collecting information on the HVAC, water, and electrical systems.

The Tier 1 screening, following the ASCE 41 checklists [5], identified the following structural deficiencies when considering the building as a C1 building type (Concrete Moment Frames) : a) column axial stress check both for IO and CP; b) column shear stress check both for IO and CP; c) flat slab frames; d) column-tie spacing; e) stirrup spacing in beams; and f) wall anchorage for out-of-plane forces. Also, the column-rebar and beam-rebar splices locations, and the joint transverse reinforcing were not identified. Furthermore, the non-structural not-compliances identified were the following: a) unreinforced masonry not braced at maximum prescriptive spacing; b) URM are not detailed to accommodate specified maximum drift ratios; c) URM working as cladding in the façades is not anchored for out-of-plane forces; d) Overhead glazing are not laminated; e) walls around stairs are not restrained for out-of-plane forces; f) the connection between the stairs and the structure relies on only one layer of four to five rebars (stair detailing); g) no flexible conduit couplings or connections; and h) no flexible fluid and gas pipping.

The exploration of the foundation discovered shallow ¨T¨ inverted grade beams. The web of the beam was 300mm in width and 1000mm depth. The flange extended 1000mm to each side of the web, resulting in 2300mm total width. The foundation is well oversized for a four-story building with 4.45m spans.

The stairs, specifically on the first story, were the most damaged element of the building. The stairs have an helicoidal shape and were built using a single layer of five-12mm rebars. This poor reinforcement, added to the eccentric location on the building plan and the inherent flexibility of the building structural system, almost caused the collapse of the first-to-second story section of the stairs. One of the 5 rebars connecting the stairs to the slab in the second story failed in tension. The stairs displaced three to five centimeters away from the slab. Considering the above, the connection between the stairs and the slabs is assumed as pinned and therefore, not considered in the analysis model.

The infill walls were constructed using clay bricks. Their dimensions were 300x140x60mm. Interestingly, the walls surrounding the stairs were built rotating the bricks a 90 degree angle, which results in 60mm as the base and not the height of each brick in the wall. All of these walls collapsed during the 2016, Muisne earthquake. Figure 2 shows the damage on the stair and the above-mentioned walls.

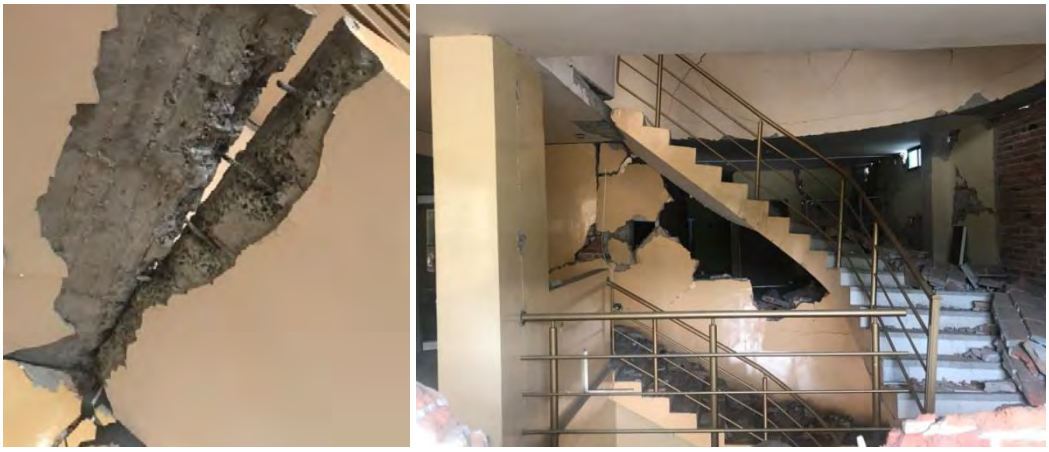

(a) (b)

Fig. 2 – (a) View from below of the connection of the stair to the slab. Notice the first bar broken and the displacement of the slab (b) Collapse of clay brick walls surrounding the helicoidal stairs.

The concrete in the building was determined to have poor strength, with an f'c in a range between 13 and 16 MPa. No original drawings or any other technical documents were found. However, the common

practice was to use a minimum compressive strength of 21 MPa. It was relatively easy to remove the cover concrete to allow the view of the rebars in the structural elements, which demonstrates the poor quality of the concrete used in the building. The previous values were obtained after extracting and testing concrete cores (15 in total) of different elements and contrasting these results with ultrasonic pulse velocity and esclerometric tests. Additionally, no corrosion in the rebars was found, both using a half-cell potential test and visual inspection when revealing the elements.

The soil was studied and classified by carrying out two exploration geotechnical probes at 15m depth, each with Standard Penetration Tests following ASTM D1586 [6] recommendations, and a geophysical prospection by microtrepidation measurements. The soil was classified, following the Unified Soil Classification System (USCS), as high plasticity silt, MH. Moreover, the Ecuadorian Construction Standard [4] follows the same site classification logic as in Table 20.3-1 of ASCE 7-16 [7]. The shear wave velocity was measured as 320 m/s, thereby, the Site Class is D. The natural period of the soil was determined to be 0.65 sec, which was also reported in the geophysical information.

The period of the structure was measured on a first testing on 05/18/2016 and almost one year later, in a second test, on 03/19/2017. Coincidentally, while the first test was being done, a month after the earthquake, the strongest recorded aftershock (MW 6.8) of the Muisne earthquake occurred. On the other hand, for the second test, the collapsed interior infill walls around the stairs, shown in figure 2.b, and some of the furniture, had been removed. The results of both tests are shown in Table 2. The transverse, T, and longitudinal, L, directions are shown in Figure 1.b. The first test results are not considered further since the aftershock altered the responses, lengthening the period in both directions. Therefore, the results in the second test are considered the base-line to compare the numerical models described in this paper. The walls around the stairs and the stairs themself were not considered in the model to reflect the actual state of the building at the moment of this second test. Furthermore, according to the Ecuadorian Construction Standard (NEC, 2015) the calculated fundamental period for the height of the building, h=12m, should have been between 0.35 sec and 0.51 sec, considering for the first value a Concrete Moment Frame System with Structural Walls and for the later, a Concrete Moment Frame without Structural Walls.

Table 2 – Ambient Vibration results of the structure

Direction	**First test (0518/2016)**	**Second test (03/19/2017)**
Transversal (**T**)	0.79	0.68
Longitudinal (**L**)	0.67	0.56
Torsion	-	0.36

5. Nonlinear model

A nonlinear model of the building was constructed using OpenSees. The infilled frames were modeled following the recommendations of chapter 11 of ASCE 41-17 [5], which in turn is partly based on the investigation of [8]. The general approach is to first classify the frame as either ductile or nonductile based on a relation between the column shear strength and the shear force corresponding to the development of plastic hinges over the column. For that, a pushover analysis of each bare frame is required. After that, the infill is categorized as weak or strong (relatively flexible and relatively stiff according to ASCE 41-17 terminology) based on the ratio between the lateral stiffness of the infill and the column flexural stiffness. Depending on the above, a specific set of equations is then used to calculate the yield, peak and residual strength, and drift. Finally, the infill-only curve would be the difference between the backbone curve of the infilled frame, calculated following the procedure described above, and the pushover curve of the bare frame. For the case-study building, twelve different infilled frames were calculated, one per story of the lateral façades (considering all the spans as 4.45m) and two per story for the back façade (considering one span of 4.10m and one of 4.70m). Different calculations for each story are required due to the increase in weight of

lower levels. That is, several single-bay, single-story models were built. Frames 1, 5, and 9 correspond to the fourth story. Frames 2, 6 and 10 correspond to the third story. Frames 3, 7 and 11 correspond to the second story. Frames 4, 8 and 12 correspond to the first floor. The classification of the different infilled frames is explained further in Figure 3. The estimated force-displacement curves for each frame are shown in Figure 4.

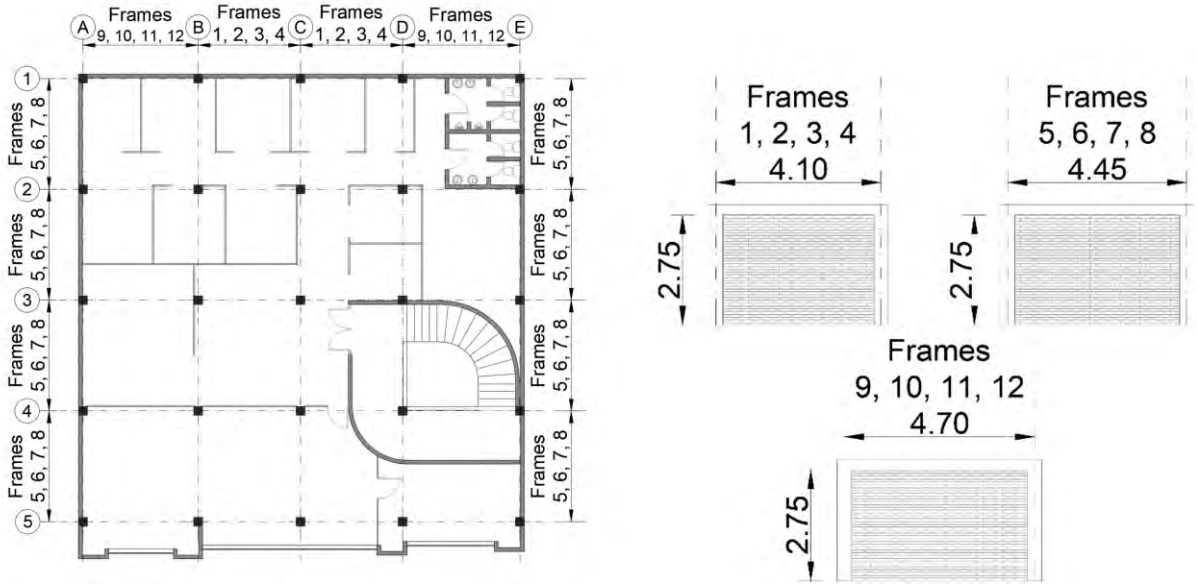

(a) (b)

Fig. 3 – (a) Classification of infilled frame, plan view (b) Infilled frame types

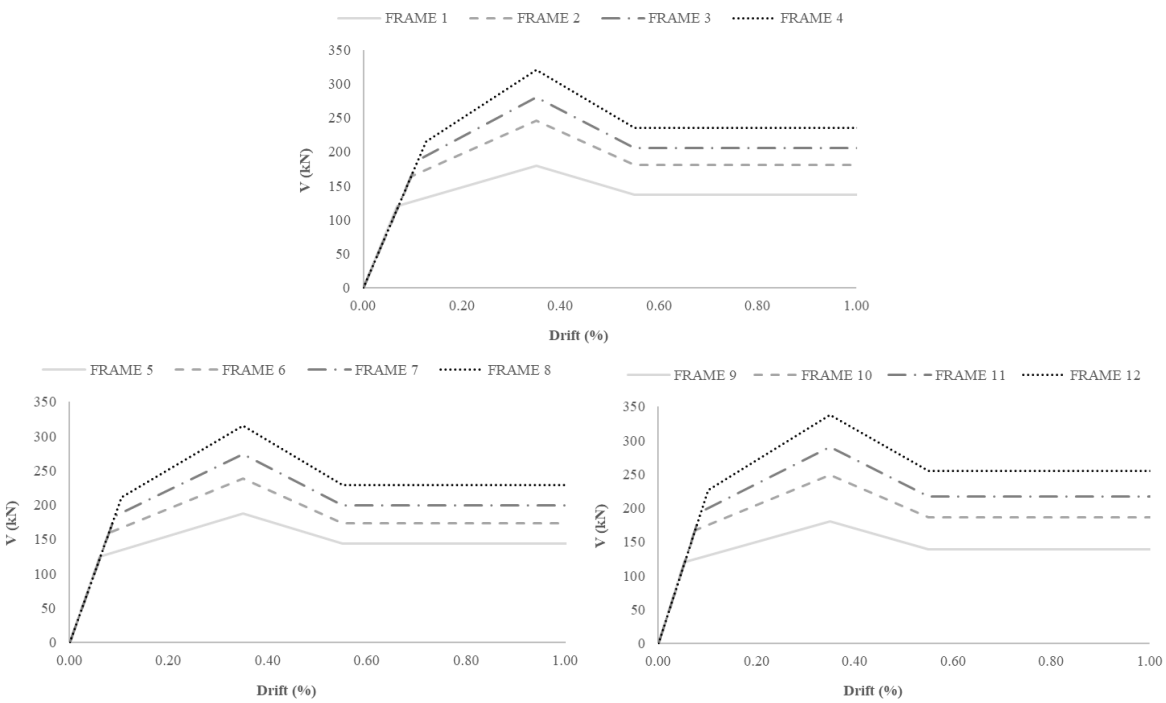

Fig. 4 – Lateral force-vs.-drift curves for the different infilled frame types

All of the infills are classified as relatively flexible. Likewise, all of the frames are classified as non-ductile. The material properties of the masonry were not directly obtained in the building but deducted from

several studies performed in Ecuador [9], [10], [11], [12] and Table 3-1 of FEMA P2018 [13] . Table 3 shows the selected values.

Table 3 – Selected Masonry Properties

f´m MPa	E'm MPa	μ0 -	μres -	C MPa
1.50	1500	0.58	0.52	0.15

One model for each single-bay, single-story infilled frame shown in Figure 3.b is built using OpenSees [14]. The masonry is represented by a diagonal strut, modeled by a truss element. The width of the strut was the same as the thickness of the wall. The height of the strut was calibrated to best approximate the backbone curves of Figure 4. Columns and beams were modeled as displacement-based inelastic beam-column elements. Both, the frame and infill, are modeled using distributed-plasticity fiber sections and Concrete02 material. Rebar is modeled using Steel02 material. Table 4 and 5 presents the material properties used for the analysis. Figure 5 compares the curves obtained following ASCE 41 and the curves calibrated using OpenSees .

Table 4 – Frame and infill Concrete02 properties used in the analysis.

Material		Peak Compressive Strength MPa	Residual Strength MPa	Tensile Strength MPa	Strain at peak strength -	Strain at residual strength -	Strut height mm	Tension Softening Stiffness MPa	Lamda
Column	Unconfined Concrete	14.0	2.3	1.8	0.0030	0.0060	-	360	0.1
	Confined Concrete	17.8	2.9	1.8	0.0031	0.0062	-	360	0.1
Beam	Unconfined Concrete	21.0	3.5	2.7	0.0030	0.0060	-	540	0.1
	Confined Concrete	26.7	4.4	2.7	0.0038	0.0076	-	540	0.1
Masonry	Strut 1	1.5	0.83	0.75	0.0017	0.0022	625	225	0.1
	Strut 2						780		
	Strut 3						975		
	Strut 4						1150		
	Strut 5						635		
	Strut 6						770		
	Strut 7						935		
	Strut 8						1100		
	Strut 9						615		
	Strut 10						770		
	Strut 11						965		
	Strut 12						1190		

Table 5 – Rebar Steel02 properties used in the analysis.

Alpha -	Yield Strength MPa	Initial elastic tangent MPa	Strain-hardening ratio -	R0 -	cR1 -	cR2 -
1.0	420	200000	0.01	18	0.925	0.15

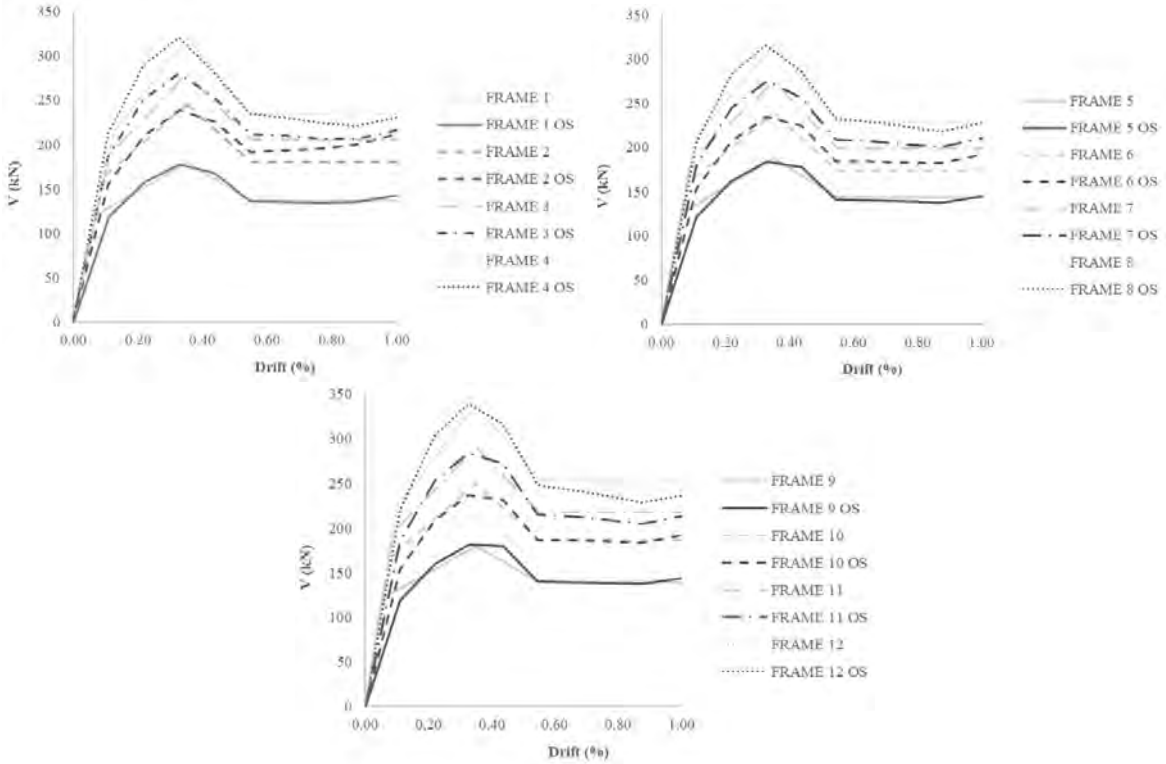

Fig. 5 – Calibrated lateral force-vs.-drift curves for the different infilled frame types

The tridimensional model is assembled using the calibrated properties of each single-bay, single-story model as shown in Table 4 and Figure 5. The two horizontal components of the recorded ground motions recorded at the station APO1 (1.038S, 80.460W) are applied to the model [2]. Fortunately, the station is located only 1.2km northwest from the case-study building.

6. Results

Table 6 compares the results from the ambient vibration tests performed in the building in March 2017, which reflect the post-earthquake state, and the results from the eigenvalue analysis of the numerical model, both before and after the application of the 2016, Muisne earthquake ground motions. The transverse, T, and longitudinal, L, directions are presented in Figure 1.b. The results are considered to be in good agreement between each other, especially for modes 1 and 3. Mode 2 results have a fair match, considering the simplicity of the modeling approach implemented.

Based on the previous results, the model is considered to be valid. Next, peak story displacements and drifts are extracted from the results of the numerical model as shown in Figure 6. The maximum displacement is about 100 mm in the roof. The maximum story drift is approximately 1%, on the second story, which coincides with the concentration of damage that was evidenced in the post-earthquake recognition.

Table 6 – Comparison of Natural Periods

Mode	Direction	Period (sec)			After EQ Error (%)
		Ambient vibration	Numerical Model		
			Before EQ	After EQ	
1	Transversal (**T**)	0.68	0.67	0.72	5.8
2	Longitudinal (**L**)	0.56	0.41	0.42	25.0
3	Torsion	0.36	0.30	0.39	8.3

At this point, a model without infills is analyzed to contrast the maximum displacement and peak story drifts of the infilled-frame and the bare-frame model. The maximum displacements in the latter reaches approximately 200mm. The maximum story drift is approximately 2%. Both the displacement and drifts double when considering bare-frames instead of infilled-frames. The post-EQ natural periods of the bare-frame model are 1.98, 1.84 and 1.59 seconds in the transversal, longitudinal and torsional modes, respectively. The magnitudes of the natural periods before the EQ for this model are 1.26, 1.22 and 1.07 seconds, following the same direction order as before. These results show a substantial degradation of the stiffness of the structure between the initial and post-earthquake state. Furthermore, the values are far from similar to the ambient vibration test results, proving this model is not able to accurately represent the actual behavior of the building. Considering the general approach, in Ecuador and several places around the world, of modeling only the bare frames, even when the masonry infills are classified as weak as in this case, the above results prove the opposite. As a result, this highlights the importance of including the infills in the analysis in order to better approximate the behavior of the structure during earthquake loading. It has been argued that infill walls, especially if categorized as weak, should not be modeled because of the loss of most of their lateral-resistance capacity only a few seconds after the beginning of an earthquake, leaving the bare-frame as the only one left to withstand the forces induced by the remaining time of the EQ. The strong portion of the Muisne earthquake lasted approximately 60 seconds, which is typical of long-duration records in subduction zones. However, for the case-study building, the infills remained, even if damaged, inside the frames until the end of the EQ. The infill walls changed dramatically, for better or worse, the behavior and response of the structure.

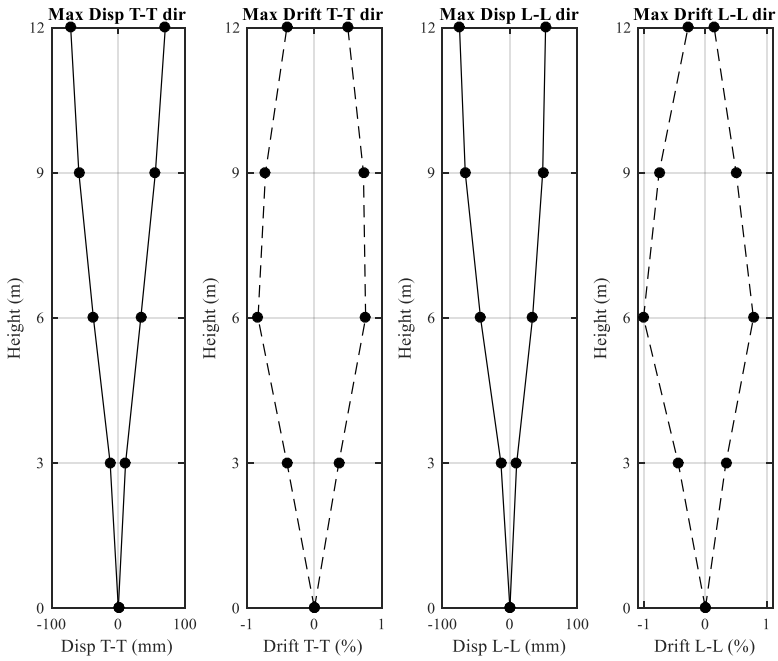

Fig. 6 – Peak story displacements and drifts

The damage state of the masonry infills is verified by contrasting the actual state of the infill walls in the post-earthquake recognition with the shear force-vs.-drift responses of each element representing the infills in the model. Figure 7 displays an elevation view of Frame 1 (back façade), following the axis notation shown in the plan view of Figure 1. Similarly, Figure 9 presents an elevation view of Frame A (side façade). Only one side façade is shown. Frame E response is similar to the one presented in Figure 9. Also, photos of the actual state of damage after the earthquake of a representative infill wall of each floor are exhibited in Figure 8. Furthermore, masonry walls in the first and fourth floor remained in good state. However, the damage concentrated in the second and third floor. Therefore, the elements that represent the infill walls in the model present a response that accurately describes the damage presented by the infills of the structure.

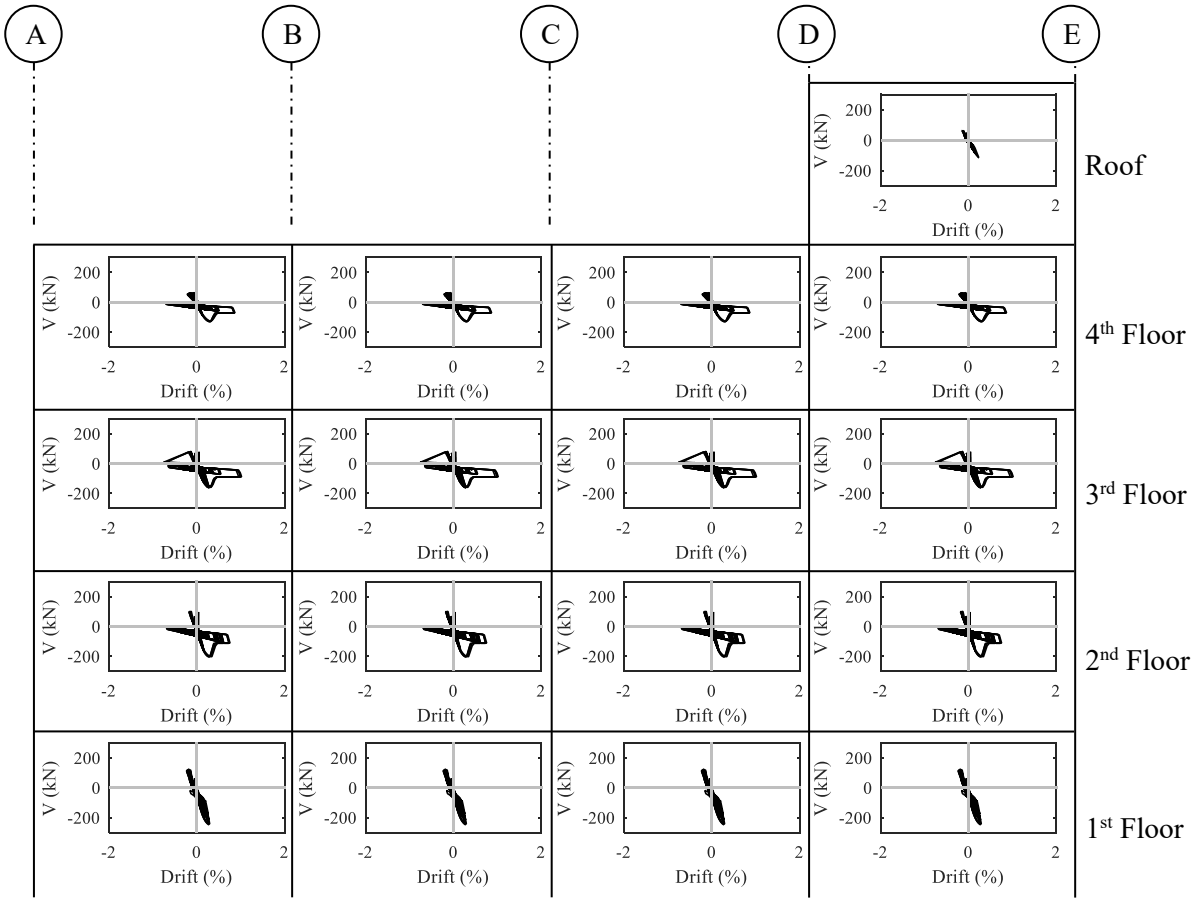

Fig. 7 – Shear force-vs.-drift plots in Frame 1 (back façade)

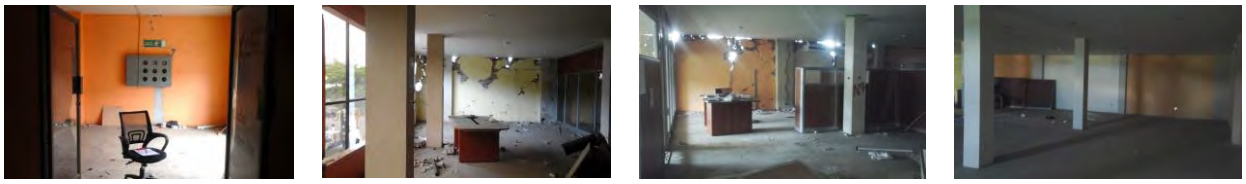

(a) 1st floor (b) 2nd floor (c) 3rd floor (d) 4th floor

Fig. 8 – Actual state of damage of masonry walls in the post-earthquake recognition

Finally, the input energy time histories of the model with and without the infills is presented in Figure 10. The contribution from each infilled frame and the total contribution from the infills is also shown.

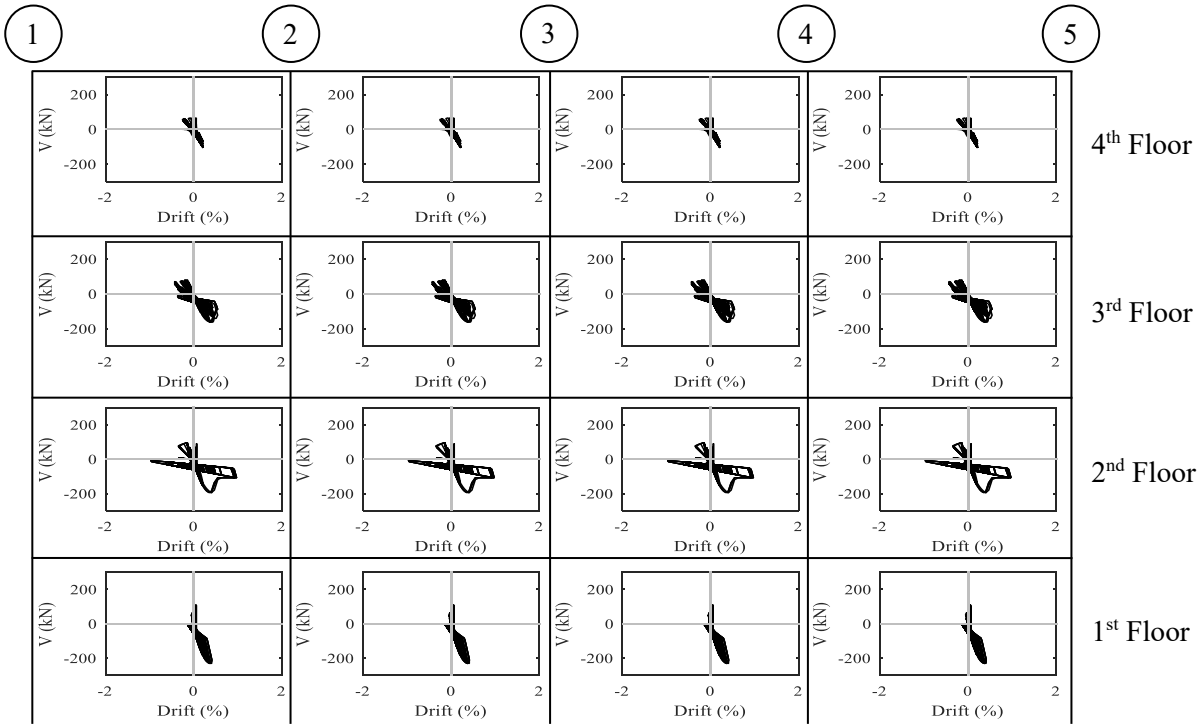

Fig. 9 – Shear force-vs.-drift plots in Frame A (side façade)

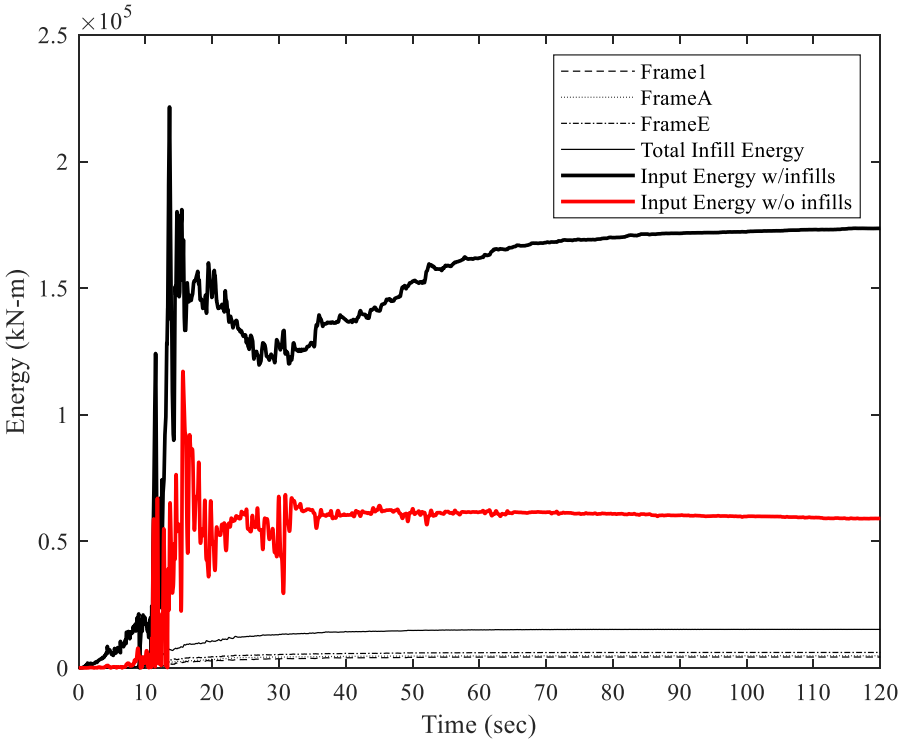

Fig. 10 – Energy Time-Histories

The amplification in the input energy for the infilled-frames model responds to the resonance effect that arose due to the similarity in the period of the soil, 0.65 sec, the period of the building, 0.67 sec, and the

predominant periods of the ground motion, between 0.30 and 0.60 secs. On the other side, the fundamental period of the bare-frames model is 1.26 seconds, distant from the soil and ground motion predominant periods. Furthermore, the contribution of the infills energy dissipation capacity is not significant.

7. Conclusions

The simplified nonlinear analysis method described in chapter 11 of ASCE 41-17 [5], [8] can accurately represent the behavior of the structure studied. The effects of the 2016, Muisne earthquake in the prototype building modify the structural behavior and this is also represented in the damaged state of the model analyzed. Previous studies [15], [16] have validated the methodology implemented in this paper to analyze the structure after an earthquake event in other parts of the world. Therefore, the method is considered to be an effective and intuitive tool to evaluate the performance of existing buildings composed of concrete moment frames and infill walls with material properties from Ecuadorian construction. Including infill walls in the analysis may change dramatically the response of the structure, for better or worse, even when the walls are, as in the case-study building, classified as weak infills.

8. Copyrights

9. References

[1] F. Lanning *et al.*, "EERI Earthquake Reconnaissance Team Report: M7.8 Muisne, Ecuador Earthquake on April 16, 2016," 2016, doi: 10.13140/RG.2.2.27341.23527.
[2] J. C. Singaucho, A. Laurendeau, C. Viracucha, and M. Ruiz, "Informe Sismico Especial N.- 18," p. 9.
[3] INEC, "Anuario de Estadísticas de Edificaciones 2014." 2014.
[4] C. S. NEC-SE-DS, "Diseno Sismo Resistente," *Norma Ecuatoriana de la Construcción*, 2015.
[5] American Society of Civil Engineers, *Seismic Evaluation and Retrofit of Existing Buildings*, 41st ed. Reston, VA: American Society of Civil Engineers, 2017.
[6] A. Standard, "D1586-11 (2011)," *ASTM D1586-11 Standard Test Method for Standard Penetration Test (SPT) and Split-Barrel Sampling of Soils, ASTM International, West Conshohocken, PA.*
[7] American Society of Civil Engineers, *Minimum Design Loads and Associated Criteria for Buildings and Other Structures*, 7th ed. Reston, VA: American Society of Civil Engineers, 2017.
[8] J. Martin and A. Stavridis, "EVALUATION OF A SIMPLIFIED METHOD FOR THE ESTIMATION OF THE LATERAL RESISTANCE OF INFILLED RC FRAMES," p. 13.
[9] L. P. Grijalva, "ELABORACIÓN DE CURVAS DE FRAGILIDAD PARA ENSAYOS EXPERIMENTALES REALIZADOS SOBRE MAMPOSTERÍAS DE BLOQUES DE CONCRETO Y LADRILLOS EN QUITO," p. 246.
[10] J. G. Vinueza, "ESTUDIO EXPERIMENTAL DE RESISTENCIA AL DESLIZAMIENTO POR CORTE EN JUNTAS DE MORTERO EN MAMPOSTERIA DE BLOQUE ARTESANAL," p. 124.
[11] R. D. Paredes, "INFLUENCIA DE LOS ELEMENTOS NO ESTRUCTURALES EN LA RESPUESTA DINÁMICA DE UN EDIFICIO. APROXIMACIÓN TEÓRICA-EXPERIMENTAL," p. 208.
[12] F. A. Pachano, "DETERMINACIÓN DE PARÁMETROS MECÁNICOS PARA MODELOS NO LINEALES DE MAMPOSTERÍA DE RELLENO EN PÓRTICOS DE HORMIGÓN ARMADO OBTENIDOS DE MANERA EXPERIMENTAL," p. 336.
[13] W. T. Holmes *et al.*, "APPLIED TECHNOLOGY COUNCIL Jon A. Heintz, Project Manager," p. 334.
[14] F. McKenna, G. L. Fenves, and F. C. Filippou, "OpenSees," *University of California, Berkeley: nd*, 2010.
[15] S. Bose, A. Nozari, A. Stavridis, and B. Moaveni, "NONLINEAR MODELING OF THE SEISMIC PERFORMANCE OF A BUILDING AT SANKHU DURING THE 2015 NEPAL EARTHQUAKE," p. 13, 2017.
[16] S. Bose and A. Stavridis, "MODELING OF THE SEISMIC PERFORMANCE OF BUILDINGS WITH INFILLED RC FRAMES," *Los Angeles*, p. 11, 2018.

